PHYSICAL REVIEW D **83,** 015008 (2011)

Technidilaton at the conformal edge

Michio Hashimoto*

Maskawa Institute for Science and Culture, Kyoto Sangyo University, Motoyama, Kamigamo, Kita-Ku, Kyoto 603-8555, Japan

Koichi Yamawaki†

Kobayashi-Maskawa Institute for the Origin of Particles and the Universe (KMI), Nagoya University, Nagoya 464-8602, Japan

(Received 5 October 2010; published 21 January 2011)

Technidilaton (TD) was proposed long ago in the technicolor near criticality/conformality. To reveal the critical behavior of TD, we *explicitly* compute the *nonperturbative* contributions to the scale anomaly $\langle\theta^\mu_\mu\rangle$ and to the technigluon condensate $\langle\alpha G^2_{\mu\nu}\rangle$, which are generated by the dynamical mass m of the technifermions. Our computation is based on the (improved) ladder Schwinger-Dyson equation, with the gauge coupling α replaced by the *two-loop running coupling* $\alpha(\mu)$ having the *Caswell-Banks-Zaks infrared fixed point* α_*: $\alpha(\mu) \simeq \alpha = \alpha_*$ for the infrared region $m < \mu < \Lambda_{\rm TC}$, where $\Lambda_{\rm TC}$ is the intrinsic scale (analogue of $\Lambda_{\rm QCD}$ of QCD) relevant to the *perturbative* scale anomaly. We find that $-\langle\theta^\mu_\mu\rangle/m^4 \to$ const $\neq 0$ and $\langle\alpha G^2_{\mu\nu}\rangle/m^4 \to (\alpha/\alpha_{\rm cr}-1)^{-3/2} \to \infty$ in the criticality limit $m/\Lambda_{\rm TC} \sim \exp(-\pi/(\alpha/\alpha_{\rm cr}-1)^{1/2}) \to 0$ ($\alpha = \alpha_* \searrow \alpha_{\rm cr}$, or $N_f \nearrow N_f^{\rm cr}$) (''conformal edge''). Our result precisely reproduces the formal identity $\langle\theta^\mu_\mu\rangle = (\beta(\alpha)/4\alpha^2)\langle\alpha G^2_{\mu\nu}\rangle$, where $\beta(\alpha) = \Lambda_{\rm TC}\frac{\partial\alpha}{\partial\Lambda_{\rm TC}} = -(2\alpha_{\rm cr}/\pi)\cdot(\alpha/\alpha_{\rm cr}-1)^{3/2}$ is the *nonperturbative* beta function corresponding to the above essential singularity scaling of $m/\Lambda_{\rm TC}$. Accordingly, the partially conserved dilatation current implies $(M_{\rm TD}/m)^2(F_{\rm TD}/m)^2 = -4\langle\theta^\mu_\mu\rangle/m^4 \to$ const $\neq 0$ at criticality limit, where $M_{\rm TD}$ is the mass of TD and $F_{\rm TD}$ the decay constant of TD. We thus conclude that at criticality limit the TD could become a ''*true (massless) Nambu-Goldstone boson*'' $M_{\rm TD}/m \to 0$, only when $m/F_{\rm TD} \to 0$, namely, getting *decoupled*, as was the case of ''holographic technidilaton'' of Haba-Matsuzaki-Yamawaki. The decoupled TD can be a candidate of dark matter.

DOI: 10.1103/PhysRevD.83.015008 PACS numbers: 11.25.Hf, 12.60.Nz, 12.60.Rc, 14.80.Va

I. INTRODUCTION

The conformal/scale-invariant (walking) technicolor (TC) characterized by the large anomalous dimension $\gamma_m = 1$ was first proposed [1,2] as a solution to the problem of the flavor-changing neutral currents (FCNC) in TC, based on the pioneering work by Maskawa and Nakajima [3] who discovered *nonzero critical coupling*, $\alpha_{\rm cr}(\neq 0)$, for the spontaneous chiral symmetry breaking (SχSB) to take place in the ladder Schwinger-Dyson (SD) equation with nonrunning (conformal) gauge coupling $\alpha(\mu) \equiv \alpha > \alpha_{\rm cr}$.[1] Subsequently, similar solution to FCNC within the same framework of the ladder SD equation was also considered without usage of the concept of the anomalous dimension [5]. See for a review, see [6].

Because of the (approximate) scale invariance, the theory also predicted [1,2] a technidilaton (TD), a composite pseudo-Nambu-Goldstone (NG) boson for the spontaneous (and explicit) breaking of the scale symmetry of the TC, as a technifermion and anti-technifermion bound state.

Actually, the mass function of the fermion $\Sigma(Q)$ of the SχSB solution takes the asymptotic form [3]

$$\Sigma(Q) \sim m^2/Q, \qquad (Q \gg m), \tag{1}$$

which was interpreted as [1]

$$\gamma_m = 1, \tag{2}$$

where the dynamical mass m ($\Sigma(m) = m$) is given by the form of essential singularity [7,8]:

$$m \sim \Lambda \cdot \exp\left(-\frac{\pi}{\sqrt{\frac{\alpha}{\alpha_{\rm cr}}-1}}\right), \qquad \alpha_{\rm cr} = \frac{\pi}{3C_F}, \tag{3}$$

with Λ being the cutoff introduced to the SD equation and C_F the quadratic Casimir of the fermion of the fundamental representation of the gauge group.

Equation (3), often called Miransky scaling, implies [8] that the dynamical generation of m by the nonperturbative dynamics should lead to the *nonperturbative* running of the coupling $\alpha = \alpha(\Lambda/m)$ ($\to \alpha_{\rm cr}$ as $\Lambda/m \to \infty$) even when it is nonrunning (conformal) in the perturbative sense:

$$\beta_{\rm NP}(\alpha) = \Lambda\frac{\partial\alpha}{\partial\Lambda} = -\frac{2\alpha_{\rm cr}}{\pi}\left(\frac{\alpha}{\alpha_{\rm cr}}-1\right)^{(3/2)}, \tag{4}$$

with $\alpha_{\rm cr}$ being interpreted as the UV fixed point. See Fig. 1 [1]. Actually, the mass scale of m has *never been created from nothing* but transferred from the ''hidden scale'' Λ

*michioh@cc.kyoto-su.ac.jp
†yamawaki@kmi.nagoya-u.ac.jp

[1]The solution of the FCNC problem by the large anomalous dimension was first considered by B. Holdom [4], based on a pure assumption of the existence of ultraviolet (UV) fixed point in TC without explicit dynamics and hence without definite prediction of the value of the anomalous dimension.

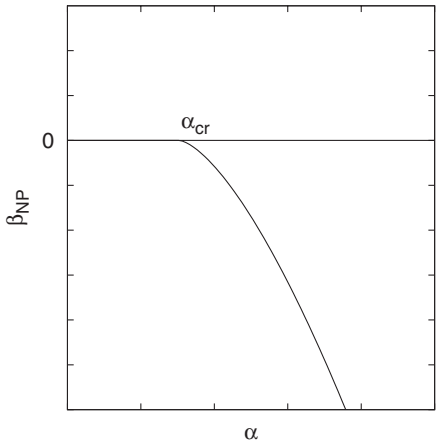

FIG. 1. Schematic behavior of the nonperturbative $\beta(\alpha)$ given in Eq. (4).

whose effect persists even when it is removed by taking the limit $\Lambda \to \infty$ while tuning $\alpha \to \alpha_{\rm cr}$.

It was then argued [2] that the dynamically generated mass m is a renormalization-group (RG)—invariant quantity, $\frac{dm}{d\mu} = 0$, and is regarded as generated by the *dimensional transmutation*:

$$m = \mu \cdot \exp\left(-\int^{\alpha(\mu)} \frac{d\alpha}{\beta_{\rm NP}(\alpha)}\right), \tag{5}$$

due to (nonperturbative) running of $\alpha(\mu)$, such that $\mu \frac{\partial \alpha(\mu)}{\partial \mu} = \beta_{\rm NP}(\alpha(\mu))$, which reflects the (nonperturbative) scale anomaly

$$\langle \partial^\mu D_\mu \rangle = \langle \theta^\mu_\mu \rangle = \frac{\beta_{\rm NP}(\alpha)}{4\alpha^2} \langle \alpha G^2_{\mu\nu} \rangle, \tag{6}$$

with $\beta_{\rm NP}(\alpha)$ given in Eq. (4), where $\langle \alpha G^2_{\mu\nu} \rangle$ is the *nonperturbative* contribution to the technigluon condensate due to the mass generation of m. Note that the nonperturbative beta function (4) has a *multiple zero*, i.e., $\beta \sim -(\alpha/\alpha_{\rm cr} - 1)^\delta$ with $\delta > 1$, which is crucial for Eq. (5) with Eq. (4) to reproduce the essential singularity scaling Eq. (3) for $\mu = \Lambda$.

Initially it was assumed [1,2] that

$$\langle \alpha G^2_{\mu\nu} \rangle = \mathcal{O}(m^4), \tag{7}$$

so that

$$\langle \theta^\mu_\mu \rangle = \beta_{\rm NP}(\alpha) \cdot \mathcal{O}(m^4), \tag{8}$$

namely, $\langle \theta^\mu_\mu \rangle / m^4 \sim \beta_{\rm NP}(\alpha) \to 0$ in the criticality limit $\alpha \to \alpha_{\rm cr}$. From the scale anomaly through partially conserved dilatation currents (PCDC), the TD mass ($M_{\rm TD}$) and its decay constant ($F_{\rm TD}$) are related as

$$M^2_{\rm TD} F^2_{\rm TD} = -4\langle \theta^\mu_\mu \rangle = -\frac{\beta_{\rm NP}(\alpha)}{\alpha^2} \langle \alpha G^2_{\mu\nu} \rangle, \tag{9}$$

which would imply $(M_{\rm TD}/m)^2 (F_{\rm TD}/m)^2 \sim -\beta_{\rm NP}(\alpha) \to 0$ for the criticality $\alpha \to \alpha_{\rm cr}$. It was then argued [2] that $M_{\rm TD}/m$ could be arbitrarily small by tuning α as $\beta_{\rm NP}(\alpha) \to 0$ ($\alpha \to \alpha_{\rm cr}$), namely, TD could become a true NG boson, $M_{\rm TD}/m \to 0$, in the criticality limit $\alpha \to \alpha_{\rm cr}$ ($m/\Lambda \to 0$).

Actually, Eq. (8) [and hence Eq. (7)] turned out to be false at least in the ladder approximation: In the criticality limit $\alpha \to \alpha_{\rm cr}$ ($m/\Lambda \to 0$) the straightforward ladder calculation [9] of $\langle \theta^\mu_\mu \rangle = 4\langle \theta^0_0 \rangle$, with the vacuum energy $\langle \theta^0_0 \rangle$ evaluated through the Cornwall-Jackiw-Tomboulis (CJT) effective potential, yields

$$\langle \theta^\mu_\mu \rangle = -4\frac{N_f N_{\rm TC}}{\pi^4} m^4, \tag{10}$$

in obvious contradiction with Eq. (8). Accordingly, we have

$$\frac{\langle \alpha G^2_{\mu\nu} \rangle}{m^4} = \frac{4\alpha^2}{\beta_{\rm NP}(\alpha)} \cdot \frac{\langle \theta^\mu_\mu \rangle}{m^4} \sim -\frac{1}{\beta_{\rm NP}(\alpha)} \to \infty, \tag{11}$$

in contrast to Eq. (7). Equation (9) now reads

$$\left(\frac{M_{\rm TD}}{m}\right)^2 \left(\frac{F_{\rm TD}}{m}\right)^2 = -\frac{4\langle \theta^\mu_\mu \rangle}{m^4} \to \text{const} \neq 0, \tag{12}$$

which implies that there is no massless TD in the criticality limit, $M_{\rm TD}/m \to \text{const} \neq 0$, as far as $m/F_{\rm TD} \to \text{const} \neq 0$.[2]

Recently a possibility was suggested [14] that the TD is relatively light compared with other technihadrons, though not extremely light: The TD mass may be evaluated at $\alpha = \alpha_{\rm cr}$ in the limit $m/\Lambda \to 0$ as

$$M_{\rm TD} \simeq \sqrt{2} m, \tag{13}$$

through the old calculation [15] of a scalar bound state in the gauged NJL model which well describes the conformal/scale-invariant gauge dynamics at criticality $\alpha \to \alpha_{\rm cr}$ where the anomalous dimension $\gamma_m = 1$ makes the induced four-fermion operator marginal with physical dimension $d = 2(3 - \gamma_m) = 4$ [10]. Equation (13) is consistent with the ladder calculation Eq. (10) [and hence Eq. (12)].

Furthermore, in the modern version [16–18] of conformal/scale-invariant TC based on the Caswell-Banks-Zaks infrared fixed point (CBZ-IRFP), $\alpha_* = \alpha_*(N_f, N_{\rm TC})$ [19], of the two-loop beta function, the coupling is almost nonrunning $\alpha(\mu) \simeq \alpha = \alpha_*$ over the wide infrared (IR) region $\mu < \Lambda_{\rm TC}$ below the intrinsic scale $\Lambda_{\rm TC}$ which is an analogue of $\Lambda_{\rm QCD}$ of QCD [see Eq. (30)]. Based on the SD equation in the (improved) ladder approximation, with the nonrunning coupling α in the ladder expression simply replaced by the two-loop running coupling $\alpha(\mu)$, we have approximately the same result as Eq. (1)–(3) with the cutoff Λ replaced by $\Lambda_{\rm TC}$ (to be typically identified with the Extended TC scale $\Lambda_{\rm ETC}$),

[2]There were several other arguments against the massless dilaton in the criticality limit of the (nearly) conformal/scale-invariant gauge theories in ladder-type approximation [10–13].

and the nonperturbative beta function Eq. (4) as well as $\gamma_m \simeq 1$ near criticality.

In this case such a relatively light TD was also suggested [14,20] from the result of the straightforward calculation [21] of scalar bound state mass,

$$M_{\rm TD} \simeq 1.5m (\simeq 4F_\pi) \simeq \sqrt{2}m < M_\rho, M_{a_1} \simeq 4.2m, \quad (14)$$

near the criticality $\alpha_* \simeq \alpha_{\rm cr}(N_f \simeq N_f^{\rm cr})$, where $N_f^{\rm cr} = N_f^{\rm cr}(N_{\rm TC})$ is determined by $\alpha_* = \alpha_{\rm cr}$ [17] and M_ρ, M_{a_1} are mass of techni-ρ and techni-a_1 mesons. The calculations are based on the SD equation and the homogeneous Bethe-Salpeter (BS) equation in the improved ladder approximation.[3] Although the result Eq. (14) is evaluated not in the critical limit $\alpha = \alpha_* \to \alpha_{\rm cr}$ but slightly away from it, the result seems to indicate $M_{\rm TD}/m \to$ const $\neq 0$ in the criticality limit $\alpha = \alpha_* \to \alpha_{\rm cr}$, which is consistent with the ladder calculation Eq. (12). Numerically, Eq. (14) suggests [14,20]

$$M_{\rm TD} \sim 500 \text{ GeV} \quad (15)$$

in the typical one-family TC model near criticality (with $N_f \simeq 4N_{\rm TC} = 8$–$12$).

More recently, TD mass was estimated by Haba, Matsuzaki and Yamawaki [23] in the hard-wall type (bottom-up) holographic approach including the technigluon condensate $\langle \alpha G_{\mu\nu}^2 \rangle$. It was found that for fixed value of S and γ_m,[4] the TD mass is a monotonically decreasing function

$$\frac{M_{\rm TD}}{m} \to 0, \qquad (\Gamma \to \infty), \quad (16)$$

of the technigluon condensate Γ (normalized by the corresponding quantity of QCD),

$$\Gamma \equiv \left(\frac{\langle \alpha G_{\mu\nu}^2 \rangle / F_\pi^4}{(\langle \alpha G_{\mu\nu}^2 \rangle / F_\pi^4)_{\rm QCD}} \right)^{(1/4)}, \quad (17)$$

where F_π is the decay constant of the (techni-) pion of order $\mathcal{O}(m)$. It was argued that the limit $\Gamma \to \infty$ is realized at the criticality $\beta_{\rm NP}(\alpha) \to 0$ ($\alpha = \alpha_* \to \alpha_{\rm cr}$), as is seen from Eq. (11), when the value of $\langle \alpha G_{\mu\nu}^2 \rangle$ is evaluated through Eq. (6) by assuming the ladder result Eq. (10) and the nonperturbative beta function Eq. (4). This would imply the existence of *true (massless) NG boson* at criticality in contrast to Eq. (13) and (possibly) Eq. (14). However, from the ladder result Eq. (12) and (16) implies that

$$\frac{m}{F_{\rm TD}} \sim \frac{M_{\rm TD}}{m} \to 0 \quad (18)$$

in that limit, namely, the holographic TD becomes a *decoupled TD* whose all couplings are characterized by the power of $(p/F_{\rm TD})$ with the typical momentum $p(\sim m)$. This is a new feature of the holographic TD.

The actual phenomenologically interesting situation of TC model building is slightly away from the criticality, $m/\Lambda = m/\Lambda_{\rm ETC} \simeq 10^{-3} - 10^{-4} \neq 0$,[5] in which case we have $\Gamma \sim 7$. This implies mass of holographic TD for typical conformal/scale-invariant TC model with $N_f \simeq 4N_{\rm TC}$ as [23]

$$M_{\rm TD} \simeq 600 \text{ GeV} < M_\rho, M_{a_1} \simeq 3.8 \text{ TeV} \quad (19)$$

for the value of $S = 0.1$ and $\gamma_m = 1$, in rough agreement with Eq. (15).[6]

Most recently, on the other hand, Appelquist and Bai [27] argued, based on the improved ladder SD equation with the two-loop running coupling, that there does exist a (nondecoupled) massless TD, $M_{\rm TD}/m \to 0$, in the conformal/scale-invariant TC in the criticality limit $\beta(\alpha) \to 0$ as $\alpha = \alpha_* \to \alpha_{\rm cr}(N_f \to N_f^{\rm cr})$, based on essentially the same assumption as in Refs. [1,2], namely, Eq. (7), which is in disagreement with the ladder calculation, Eq. (10), as noted before. (See also Ref. [28].) Note that although the beta function in Ref. [27] is somewhat different from that in Eq. (4) used in Ref. [2], they both vanish at the criticality $\alpha_* \to \alpha_{\rm cr}$ ($N_f \to N_f^{\rm cr}$).

In view of these subtleties in the literature on the critical behavior of the TD near the conformal edge associated with the CBZ-IRFP, it is very important to settle the critical behavior of $\langle \alpha G_{\mu\nu}^2 \rangle$ and $\langle \theta_\mu^\mu \rangle$ in the calculation within the same framework as that relevant to the above controversy, namely, literally *incorporating the perturbative two-loop running effects* as well the nonperturbative effects which produce the dynamical mass m.

In this paper we shall explicitly calculate the nonperturbative contributions to the technigluon condensate $\langle \alpha G_{\mu\nu}^2 \rangle$ and to the scale anomaly $\langle \theta_\mu^\mu \rangle = 4\langle \theta_0^0 \rangle$ arising from the fermion mass generation in the TC near conformality/criticality (conformal edge), $\alpha_* \to \alpha_{\rm cr}(N_f \to N_f^{\rm cr})$, based on the "improved ladder SD equation" [29]. Although the improved ladder approximation with the two-loop running coupling as well as the ladder approximation with nonrunning coupling is not a systematic approximation and hence not very reliable, all the above controversy about the

[3]These results are compared with those in QCD: [22] $(M_\rho/F_\pi)/(M_\rho/F_\pi)_{\rm QCD} \simeq 1.3$, $(M_{a_1}/F_\pi)/(M_{a_1}/F_\pi)_{\rm QCD} \simeq 0.86$, while $(M_{\rm TD}/F_\pi)/(M_{\rm scalar}/F_\pi)_{\rm QCD} \simeq 0.38$.

[4]Note that in the holography the S parameter [24] and anomalous dimension γ_m are not calculable parameters but arbitrary adjustable parameters [25].

[5]In the actual situation of TC, m is the weak scale $m \sim$ TeV and Λ is identified with the typical scale $\Lambda_{\rm ETC}$ of the dynamics [like the extended TC (ETC)] transmitting the technifermion mass m to that of the quark/lepton, i.e., $\Lambda = \Lambda_{\rm ETC} \sim 10^3$ TeV. Thus $m/\Lambda \sim 10^{-3} - 10^{-4}$ which corresponds to $\beta(\alpha) \gtrsim 10^{-2}$ (for $N_{\rm TC} = 2$–3) from Eqs. (3) and (4).

[6]The value M_ρ, M_{a_1} is essentially determined by the value of S: Lower S value corresponds to higher M_ρ, M_{a_1}. The calculated S value in Ref. [26] in the same setting as Ref. [21] is higher than $S = 0.1$, which corresponds to the value of M_ρ, M_{a_1} in the holography close to that of Eq. (14).

technidilaton in the literature has been confined to this approximation. So our aim of this paper is to resolve the confusion within this approximation. We first study analytically the solution of the improved ladder SD equation, with the two-loop running coupling being approximated by a simplified ansatz (solution to the ''parabolic'' beta function $\beta(\alpha) = -b_0\alpha(\alpha_* - \alpha)$),

$$\alpha(\mu^2) = \frac{\alpha_*}{1 + e^{-1}(\frac{\mu^2}{\Lambda_{\rm TC}^2})^{b_0\alpha_*}}, \tag{20}$$

which agrees with the exact two-loop running coupling written in terms of the Lambert's W function in the IR region $\mu < \Lambda_{\rm TC}$ responsible for the dynamical mass generation (see text). The result will be checked by the numerical solution based on the exact two-loop running coupling.

We then calculate the technigluon condensate near the conformal edge and show explicitly it behaves as $\langle G_{\mu\nu}^2\rangle/m^4 \sim (\alpha/\alpha_{\rm cr} - 1)^{-3/2} \to \infty$ $(\alpha \to \alpha_{\rm cr})$, which is a direct evidence against the assumption of Ref. [2] (in the ladder SD equation with nonrunning coupling) and also that of Ref. [27] (in the improved ladder SD equation with the two-loop running coupling). Our result directly confirms the estimate of the technigluon condensate in Ref. [23] which indicates divergence of the technigluon condensate $\Gamma \to \infty$ at criticality.

We also find that the numerical calculation of the vacuum energy with the two-loop running coupling agrees with the analytical solution (10) with the fixed coupling, $\langle\theta_\mu^\mu\rangle \sim -m^4$, again in contrast to the assumption in Ref. [2] and Ref. [27].

On the other hand, the scale anomaly satisfies the formal relation, $\langle\theta_\mu^\mu\rangle = \beta(\alpha)/(4\alpha)\cdot\langle G_{\mu\nu}^2\rangle$. Hence our results imply the beta function near criticality:

$$\beta(\alpha) = \frac{4\alpha\langle\theta_\mu^\mu\rangle}{\langle G_{\mu\nu}^2\rangle} \sim -\left(\frac{\alpha}{\alpha_{\rm cr}} - 1\right)^{(3/2)}. \tag{21}$$

The result also confirms the assumption made in Ref. [23] where the nonperturbative beta function, Eq. (4), as well as the ladder result of the vacuum energy was used for the nonperturbative conformal anomaly to estimate the technigluon condensate.

We thus conclude that the nonperturbative beta function arising from the nonperturbative effects of the dynamical mass generation in the IR region $(\mu < \Lambda_{\rm TC})$ is essentially like Eq. (4), Fig. 1, even in the case of the two-loop running gauge coupling set in the SD equation. It should be considerably changed from the perturbative expression near criticality. In Fig. 14, we schematically depict the conjectured behavior of the beta function including both of the perturbative and nonperturbative region.

Our two-loop results combined with the PCDC relation, $F_{\rm TD}^2 M_{\rm TD}^2 = -4\langle\theta_\mu^\mu\rangle \sim m^4$, suggest $F_{\rm TD}^2/m^2 \cdot M_{\rm TD}^2/m^2 \to$ finite at the critical point, which is the same as the nonrunning case (12); There is no theoretically controllable suppression factor for $M_{\rm TD}/m \to 0$, as far as $F_{\rm TD}/m$ is finite. This contradicts the assumptions in Ref. [2] and Ref. [27]. However, our results cannot exclude the possibility [the ''decoupled TD,'' Eqs. (16) and (18)] that there might exist a very light TD, $M_{\rm TD} \sim 0$, if $F_{\rm TD}/m$ is quite large, as could be the case in the limit of the holographic TD [23]. This decoupled TD may be dark matter.

This paper is organized as follows: In Sec. II, we describe the behavior of the beta function in the two-loop approximation. We also introduce the parabolic approximation in order to solve analytically the improved ladder SD equation. In Sec. III, we study the analytical solution of the SD equation in the parabolic approximation and also analyze the numerical solution with the two-loop exact gauge coupling. We show that the approximation works well. Then we calculate the technigluon condensate and the vacuum energy. Section IV is devoted for summary and discussions.

II. TWO-LOOP β FUNCTION AND PARABOLIC APPROXIMATION

In this section, we study the running effect of the gauge coupling constant in the two-loop approximation. It is well-known that there appears the CBZ-IRFP [19], when the number of (techni-)fermions is in a certain range, as we will show later. If the value of the CBZ-IRFP α_* slightly exceeds the critical coupling $\alpha_{\rm cr}$ for the SχSB, we can apply such gauge theories to the TC with near conformality with anomalous dimension $\gamma_m \simeq 1$ [16–18]. We here employ the approach of the (improved) ladder SD equation [29], with the nonrunning coupling in the ladder SD equation simply replaced by the running one, this time the two-loop running coupling. Although the numerical analysis of the (improved) ladder SD equation is rather straightforward, it is not so easy to extract numerically the critical behavior of the solution. We thus approximate the two-loop β function into a parabolic one and will solve *analytically* the ladder SD equation. In the next section, we will demonstrate that this approximation works very well.

Let us study the two-loop renormalization group equation for the gauge coupling constant α [30]:

$$\mu\frac{\partial}{\partial\mu}\alpha = \beta(\alpha) = -b_0\alpha^2 - b_1\alpha^3, \tag{22}$$

with

$$b_0 = \frac{1}{6\pi}(11C_A - 4N_f T_R), \tag{23}$$

and

$$b_1 = \frac{1}{12\pi^2}[17C_A^2 - 2N_f T_R(5C_A + 3C_F)], \tag{24}$$

where N_f represents the number of flavor and the group theoretical factors are

$$C_A = N_{\rm TC}, \qquad T_R = \frac{1}{2}, \qquad C_F = \frac{N_{\rm TC}^2 - 1}{2N_{\rm TC}}, \tag{25}$$

for $SU(N_{\rm TC})$ gauge theories.

When $b_0 > 0$ and $b_1 < 0$, i.e.,

$$\frac{34N_{\rm TC}^3}{13N_{\rm TC}^2 - 3} < N_f < \frac{11}{2}N_{\rm TC}, \tag{26}$$

the CBZ-IRFP α_* emerges,

$$\alpha_* = \frac{b_0}{-b_1}. \tag{27}$$

The analytic form of $\alpha(\mu^2)$ is also known [31]:

$$\alpha(\mu^2) = \frac{\alpha_*}{1 + W(z(\mu^2))}, \tag{28}$$

where W denotes the Lambert function [32], which is the inverse of xe^x, and z is defined by

$$z(\mu^2) \equiv \frac{1}{e}\left(\frac{\mu^2}{\Lambda_{\rm TC}^2}\right)^{b_0\alpha_*}, \tag{29}$$

where the intrinsic scale $\Lambda_{\rm TC}$ analogous to $\Lambda_{\rm QCD}$ invariant under renormalization group equation is given by [17]:

$$\begin{aligned}\Lambda_{\rm TC} &= \mu \cdot \exp\left(\int^{\alpha(\mu)} \frac{d\alpha}{\beta(\alpha)}\right) \\ &= \mu \cdot \exp\left[-\frac{1}{b_0\alpha(\mu^2)} - \frac{1}{b_0\alpha_*}\ln\left(\frac{\alpha_* - \alpha(\mu^2)}{\alpha(\mu^2)}\right)\right],\end{aligned} \tag{30}$$

with the first term in $[\ldots]$ being the usual one-loop contribution and the second the two-loop one. We can, of course, rescale $\Lambda_{\rm TC}$ freely. Here we chose $\Lambda_{\rm TC}$ as

$$\Lambda_{\rm TC}:\ \alpha(\mu^2 = \Lambda_{\rm TC}^2) = \frac{\alpha_*}{1 + W(e^{-1})} \simeq 0.78\alpha_*, \tag{31}$$

which reflects the conformal anomaly associated with the perturbative running in the UV region $\mu > \Lambda_{\rm TC}$ dominated by the one-loop effects,

$$\partial_\mu D^\mu|_{\rm perturbative} = \frac{\beta(\alpha)}{4\alpha^2}(\alpha G_{\mu\nu}^2)|_{\rm perturbative} = \mathcal{O}(\Lambda_{\rm TC}^4), \tag{32}$$

while keeping the (approximate) conformal symmetry (via (almost) nonrunning coupling) in the IR region $\mu < \Lambda_{\rm TC}$ so as to be broken only nonperturbatively by the dynamical generation of the technifermion mass m. Actually, the UV and IR behaviors of $\alpha(\mu^2)$ in Eq. (28) are

$$\alpha(\mu^2) \approx \frac{1}{b_0 \ln\frac{\mu^2}{\Lambda_{\rm TC}^2}} \qquad (\mu^2 \gg \Lambda_{\rm TC}^2), \tag{33}$$

and

$$\alpha(\mu^2) \approx \frac{\alpha_*}{1 + e^{-1}\left(\frac{\mu^2}{\Lambda_{\rm TC}^2}\right)^{b_0\alpha_*}}, \qquad (\mu^2 \ll \Lambda_{\rm TC}^2), \tag{34}$$

respectively.

Note that in this paper we are not interested in the perturbative part of the conformal anomaly in Eq. (32) and will focus on the *nonperturbative* contributions to the conformal anomaly and the relevant technigluon condensate associated with the dynamical generation of the mass m in the IR dynamics: [9,23]

$$\begin{aligned}\langle \alpha G_{\mu\nu}^2 \rangle &\equiv \langle \alpha G_{\mu\nu}^2 \rangle_{\rm full} - \langle \alpha G_{\mu\nu}^2 \rangle_{\rm perturbative}, \\ \langle \theta_\mu^\mu \rangle &\equiv \langle \theta_\mu^\mu \rangle_{\rm full} - \langle \theta_\mu^\mu \rangle_{\rm perturbative},\end{aligned} \tag{35}$$

where the perturbative conformal anomaly $\langle \theta_\mu^\mu \rangle_{\rm perturbative} = -\mathcal{O}(\Lambda_{\rm TC}^4)$ is associated with the perturbative running effects of the coupling in the UV region $\mu > \Lambda_{\rm TC}$. The quantities defined in Eq. (35) are similar to those discussed in Ref. [27].

In order to solve *analytically* the improved ladder SD equation, we would need to simplify the expression of α. We thus adopt the approximation (34) in *all* region, because it enjoys both of desirable natures, the CBZ-IRFP ($\alpha \to \alpha_*$ for $\mu \to 0$) and the asymptotic freedom ($\alpha \to 0$ for $\mu \to \infty$). This approximation corresponds to a parabolic β function,

$$\beta(\alpha) = -b_0\alpha(\alpha_* - \alpha), \tag{36}$$

which can be applied from the IR region to the UV region. Although the damping of α in the UV region is much faster than the two-loop solution (28), [see Fig. 3] it turns out that the critical behavior of the dynamical mass is insensitive to the UV behavior of the mass function. On the other hand, the linear approximation $\beta(\alpha) = -b_0\alpha_*(\alpha_* - \alpha)$, which yields $\alpha(\mu^2) = \alpha_*(1 - e^{-1}(\mu^2/\Lambda_{\rm TC}^2)^{b_0\alpha_*})$, is simpler, but it can be applied only in a narrower region.

Schematic behaviors of the two-loop and parabolic β functions are depicted in Fig. 2. We also show the running effects of the gauge coupling α for both cases in Fig. 3, where we took $N_{\rm TC} = 3$ and $N_f = 11.85$ ($\alpha_* = 0.810$). The parabolic approximation is very successful in the IR

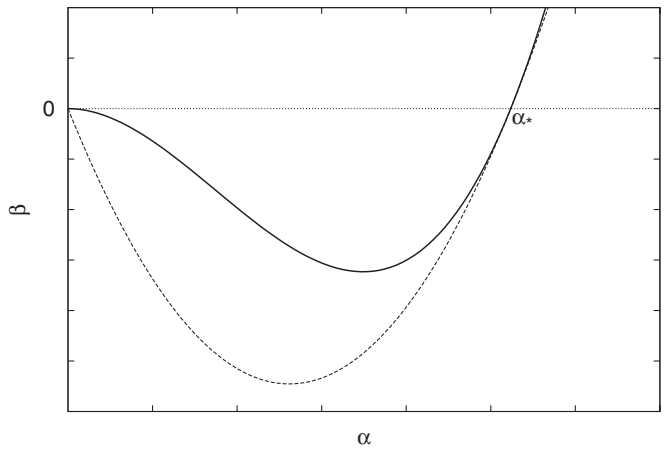

FIG. 2. Behavior of $\beta(\alpha)$ in perturbation. The bold solid and dashed curves correspond to the two-loop β function (22) and the parabolic one (36), respectively.

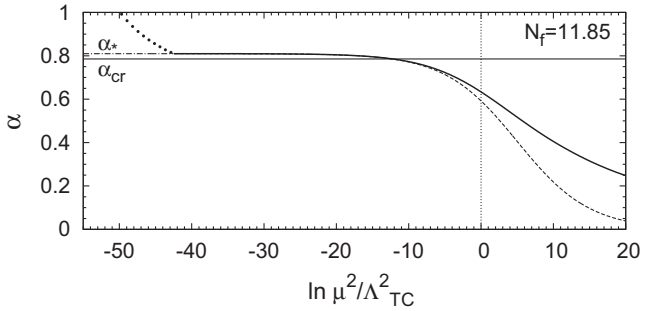

FIG. 3. Behavior of α. The bold solid and dashed curves correspond to the behavior of α for the two-loop β function (22) and the parabolic approximation (36). We took $N_{\rm TC} = 3$ and $N_f = 11.85$, which yields $\alpha_* = 0.810$. The scale $\alpha(\mu^2 = \mu^2_{\rm cr}) = \alpha_{\rm cr} = \pi/4$ is given by $\mu_{\rm cr}/\Lambda_{\rm TC} = 0.002\,25$. Below the scale of the dynamical mass m, numerically $m/\Lambda_{\rm TC} = 5.88 \times 10^{-10}$ obtained by solving the corresponding ladder SD equation with the gauge coupling (28), the technifermions should be decoupled and thereby the running of α is expected to be changed. The dots below $\mu < m$ corresponds to this expectation. The dash-dotted curve below $\mu < m$ is for the formal solution of the two-loop β function.

region $\mu \lesssim \Lambda_{\rm TC}$, while the damping of α is quicker than the two-loop one in the UV region $\mu \gg \Lambda_{\rm TC}$, as we mentioned above. (See Fig. 3.) Below the scale of the dynamical mass m discussed in the next section, the technifermions should be decoupled and thereby the running of α is expected to be changed. We depict this expectation by the dots below $\mu < m$ in Fig. 3.

III. ANALYSIS OF THE LADDER SD EQUATION WITH RUNNING GAUGE COUPLING CONSTANTS

A. The CJT potential and the improved ladder SD equation

The ladder SD approach is a convenient method to analyze the dynamical generation of the fermion mass and its critical behavior. In order to incorporate the running effect of the gauge coupling α, a conventional technique, so-called the improved ladder approximation, has been widely employed [29]. We can derive the improved ladder SD equation via the CJT potential $V_{\rm CJT}$ [33]:

$$V_{\rm CJT}(B) = -\frac{N_{\rm TC}N_f}{4\pi^2}\Bigg[\int_0^{\Lambda^2} dx x \times \left\{\frac{1}{2}\ln\left(1+\frac{B^2(x)}{x}\right) - \frac{B^2(x)}{x+B^2(x)}\right\} + \frac{1}{2}\int_0^{\Lambda^2} dx x \int_0^{\Lambda^2} dy y \frac{B(x)B(y)}{(x+B^2(x))(y+B^2(y))} \times \left(\frac{\lambda(x)}{x}\theta(x-y) + \frac{\lambda(y)}{y}\theta(y-x)\right)\Bigg], \quad (37)$$

with the (normalized) gauge coupling $\lambda(x)$,

$$\lambda(x) \equiv \frac{3C_F\alpha(\mu^2 = x)}{4\pi}, \quad (38)$$

where x and y denote the Euclidean momenta, the full fermion propagator inverse is $iS_f^{-1}(p) = A(-p^2)\not{p} - B(-p^2)$, and we took the Landau gauge at which the fermion wave function renormalization is unity, $A(-p^2) \equiv 1$. See Fig. 4. Although the UV cutoff Λ is not needed for case of the two-loop running coupling which is asymptotically free in the UV region in contrast to the nonrunning case, we have put an artificial $\Lambda(\to \infty)$ in Eq. (37) only for the numerical calculation, which should not be confused with Λ in the nonrunning case used in Eqs. (3) and (4). The variation of $V_{\rm CJT}$ with respect to the fermion mass function $B(x)$ with $x \equiv -p^2$ yields the improved ladder SD equation [33],

$$B(x) = \int_0^{\Lambda^2} dy \frac{yB(y)}{y+B^2(y)}\left[\frac{\lambda(x)}{x}\theta(x-y) + \frac{\lambda(y)}{y}\theta(y-x)\right]. \quad (39)$$

B. Analytic solution for the improved ladder SD equation in the parabolic approximation

The integral Eq. (39) is equivalent to a set of a nonlinear differential equation and boundary conditions (BC's). It is, however, difficult to solve *analytically* the nonlinear differential equation in general. We may adopt the bifurcation method [34], which yields a more handy linearized differential equation. We also ignore $xd\lambda/dx \propto \beta$, because of $\beta \sim 0$ near $x \sim 0$ and $x \sim \infty$. Under these simplifications, we obtain the following differential equation and the two BC's:

$$x^2\frac{d^2}{dx^2}B(x) + 2x\frac{d}{dx}B(x) + \frac{\lambda_*}{1+e^{-1}\left(\frac{x}{\Lambda^2_{\rm TC}}\right)^s}B(x) = 0, \quad (40)$$

and

$$\text{(UV-BC): } x\frac{d}{dx}B(x)|_{x=\Lambda^2} + B(\Lambda^2) = 0, \quad (41)$$

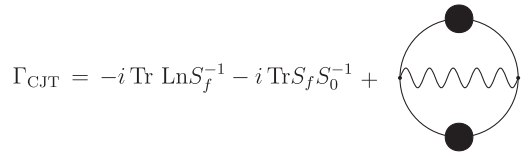

FIG. 4. Effective action for the fermion propagator. The CJT potential is defined by $\Gamma_{\rm CJT} = -V_{\rm CJT}\int dx^4$. S_f and S_0 represent the full fermion propagator and the free one, respectively. In the last diagram, the solid line with a shaded blob and the wavy line represent the full fermion propagator S_f and the gauge boson propagator, respectively.

$$\text{(IR-BC): } x^2 \frac{d}{dx} B(x)|_{x\to m^2} \to 0, \tag{42}$$

where m is defined by the normalization of the mass function,

$$B(x = m^2) = m, \tag{43}$$

and the IRFP λ_* and the power factor s are

$$\lambda_* \equiv \frac{3C_F \alpha_*}{4\pi}, \tag{44}$$

and

$$s \equiv b_0 \alpha_* > 0, \tag{45}$$

respectively. In the parabolic approximation, the normalized gauge coupling $\lambda(x)$ is

$$\lambda(x) = \frac{\lambda_*}{1 + e^{-1}\left(\frac{x}{\Lambda_{\rm TC}^2}\right)^s}. \tag{46}$$

Note that in the limit of $s \to \infty$ the gauge coupling becomes $\lambda(x) = \lambda_* \theta(e^{(1/s)}\Lambda_{\rm TC}^2 - x)$, where the step function is defined by $\theta(t) = 1$ for $t > 0$, $\theta(t) = 1/2$ for $t = 0$, and $\theta(t) = 0$ for $t < 0$.

We can *analytically* solve the differential Eq. (40) as follows:

$$\begin{aligned}\frac{B(x)}{m} &= c_1 \left(\frac{x}{m^2}\right)^{-(1-\omega)/2} \\ &\times F\left(-\frac{1-\omega}{2s}, -\frac{-1-\omega}{2s}, 1 + \frac{\omega}{s}; -\bar{x}^s\right) \\ &+ d_1 \left(\frac{x}{m^2}\right)^{-(1+\omega)/2} \\ &\times F\left(-\frac{1+\omega}{2s}, -\frac{-1+\omega}{2s}, 1 - \frac{\omega}{s}; -\bar{x}^s\right), \quad (x \geq m^2),\end{aligned} \tag{47}$$

where $F(\alpha, \beta, \gamma; z)$ represents the Gauss's hypergeometric function[7] and we introduced

$$\bar{x} \equiv e^{-1/s} \frac{x}{\Lambda_{\rm TC}^2}, \tag{48}$$

and

$$\omega \equiv \sqrt{1 - \frac{\lambda_*}{\lambda_{\rm cr}}}, \qquad \lambda_{\rm cr} \equiv \frac{1}{4}. \tag{49}$$

The integration constants c_1 and d_1 are determined through the IR-BC and the normalization of $B(x)$. The UV-BC gives the scaling relation.

[7]If we employ the linear approximation, $\lambda(x) = \lambda_*(1 - e^{-1}(x/\Lambda_{\rm TC}^2)^s)$, the analytical solution is written by the modified Bessel functions.

The normalization $B(x = m^2) = m$ yields

$$\begin{aligned}1 = c_1 F&\left(-\frac{1-\omega}{2s}, -\frac{-1-\omega}{2s}, 1 + \frac{\omega}{s}; -\bar{x}_m^s\right) \\ &+ d_1 F\left(-\frac{1+\omega}{2s}, -\frac{-1+\omega}{2s}, 1 - \frac{\omega}{s}; -\bar{x}_m^s\right),\end{aligned} \tag{50}$$

with

$$\bar{x}_m \equiv e^{-1/s} \frac{m^2}{\Lambda_{\rm TC}^2}. \tag{51}$$

On the other hand, the IR-BC gives

$$\begin{aligned}c_1 \Bigg[&\omega F\left(-\frac{1-\omega}{2s}, -\frac{-1-\omega}{2s}, 1 + \frac{\omega}{s}; -\bar{x}_m^s\right) \\ &+ \frac{\lambda_*}{s+\omega} \bar{x}_m^s F\left(1 - \frac{1-\omega}{2s}, 1 + \frac{1+\omega}{2s}, 2 + \frac{\omega}{s}; -\bar{x}_m^s\right)\Bigg] \\ &+ d_1 \frac{\lambda_*}{s-\omega} \bar{x}_m^s F\left(1 - \frac{1+\omega}{2s}, 1 + \frac{1-\omega}{2s}, 2 - \frac{\omega}{s}; -\bar{x}_m^s\right) \\ &= \frac{1+\omega}{2},\end{aligned} \tag{52}$$

where we used Eq. (50).

In the limit of $m \ll \Lambda_{\rm TC}$, we obtain

$$c_1 = \frac{1+\omega}{2\omega}, \qquad d_1 = -\frac{1-\omega}{2\omega}, \tag{53}$$

which corresponds to the coefficients of the bifurcation solution with the fixed gauge coupling $\lambda(x) = \lambda_*$. On the other hand, the UV-BC in the limit of $m^2 \ll \Lambda_{\rm TC}^2 \ll \Lambda^2$ yields

$$\left(\frac{e^{1/s}\Lambda_{\rm TC}^2}{m^2}\right)^\omega = \frac{(1-\omega)^2}{(1+\omega)^2} \frac{\Gamma(1 - \frac{\omega}{s})\Gamma^2(1 + \frac{1+\omega}{2s})}{\Gamma(1 + \frac{\omega}{s})\Gamma^2(1 + \frac{1-\omega}{2s})}. \tag{54}$$

It is noticeable that the dependence of the UV cutoff Λ disappears. Only when ω is pure imaginary, i.e.,

$$\lambda_* > \lambda_{\rm cr} = \frac{1}{4}, \tag{55}$$

Equation (54) has a relevant solution,

$$\ln \frac{m}{e^{1/(2s)}\Lambda_{\rm TC}} = -\frac{n\pi}{\tilde{\omega}} + \frac{2\arctan\tilde{\omega}}{\tilde{\omega}} - \frac{\ln\left[\frac{\Gamma(1 - \frac{i\tilde{\omega}}{s})\Gamma^2(1 + \frac{1+i\tilde{\omega}}{2s})}{\Gamma(1 + \frac{i\tilde{\omega}}{s})\Gamma^2(1 + \frac{1-i\tilde{\omega}}{2s})}\right]}{2i\tilde{\omega}}, \tag{56}$$

where

$$\tilde{\omega} \equiv \sqrt{\frac{\lambda_*}{\lambda_{\rm cr}} - 1}, \tag{57}$$

and $n = 1, 2, 3, \cdots$. It is known that the zero node solution $n = 1$ is the true vacuum [33]. Equation (56) yields the essential singularity scaling relation,

$$m \sim e^{-\pi/\tilde{\omega}} \Lambda_{\rm TC} = \Lambda_{\rm TC} \cdot \exp\left(-\frac{\pi}{\sqrt{\frac{\alpha_*}{\alpha_{\rm cr}} - 1}}\right), \tag{58}$$

similarly to Eq. (3) with replacement of α by α_* and Λ by $\Lambda_{\rm TC}$.

The behavior of the mass function $B(x)$ in the supercritical region $\lambda_* > \lambda_{\rm cr}$ is approximately

$$\frac{B(x \ll \Lambda_{\rm TC}^2)}{m} \simeq \frac{\sqrt{1+\tilde{\omega}^2}}{\tilde{\omega}} \left(\frac{x}{m^2}\right)^{-1/2} \times \sin\left[\frac{\tilde{\omega}}{2} \ln\left(\frac{x}{m^2}\right) + \arctan\tilde{\omega}\right], \quad (59)$$

$$\frac{B(x \gg \Lambda_{\rm TC}^2)}{m} \simeq e^{1/2s}[A(\tilde{\omega}) + A(-\tilde{\omega})]\frac{m\Lambda_{\rm TC}}{x}, \quad (60)$$

with

$$A(\tilde{\omega}) \equiv \frac{\lambda_*}{i\tilde{\omega}} \frac{\Gamma(1+\frac{i\tilde{\omega}}{s})\Gamma(1-\frac{1}{s})}{\Gamma^2(1+\frac{-1+i\tilde{\omega}}{2s})} \left(\frac{e^{1/(2s)}\Lambda_{\rm TC}}{m}\right)^{i\tilde{\omega}}. \quad (61)$$

The behaviors of the mass function in the IR and UV regions correspond to those with the anomalous dimensions $\gamma_m = 1$ and $\gamma_m = 0$, respectively. In particular, owing to the quicker damping of α than the logarithm, there is no log correction unlike QCD. On the other hand, the IR behavior is the same as that for the fixed coupling.

In passing, the critical number N_f, which corresponds to $\lambda_{\rm cr}$, is

$$N_f^{\rm cr} = 4N_{\rm TC}\left[1 - \frac{3}{10}\frac{1}{5N_{\rm TC}^2 - 3}\right]. \quad (62)$$

Since the power factor s is

$$s = b_0\alpha_* = \frac{(11N_{\rm TC} - 2N_f)^2}{-6[17N_{\rm TC}^2 - N_f(5N_{\rm TC} + 3C_F)]}, \quad (63)$$

at the critical point, it reads

$$s_{\rm cr} = b_0\alpha_{\rm cr} = \frac{N_{\rm TC}}{18(N_{\rm TC}^2 - 1)}\left[3N_{\rm TC} + \frac{12}{5}\frac{N_{\rm TC}}{5N_{\rm TC}^2 - 3}\right]. \quad (64)$$

For $N_{\rm TC} = 3$, they are numerically

$$N_f^{\rm cr} = \tfrac{417}{35} \simeq 11.914, \qquad s_{\rm cr} = \tfrac{107}{560} \simeq 0.191\,02. \quad (65)$$

We can solve numerically the improved-ladder SD Eq. (39) with the normalized gauge coupling (46). The computational technique is described in Ref. [35].

We depict the analytical and numerical solutions of $B(x)$ in Fig. 5, where we took $N_{\rm TC} = 3$ and $N_f = 11.63$. Although we drastically simplified the integral Eq. (39) into the linearized differential Eq. (40) with the two BC's, we find that the approximation works well.

The scaling relations in the numerical and analytical approaches are shown as the dashed and dotted curves in Fig. 6, respectively. We confirmed that the numerical solution is unchanged for $\Lambda/\Lambda_{\rm TC} = 10^{1,2,\cdots,10}$. (It is not the case for $\Lambda = \Lambda_{\rm TC}$, however.) In the figure, we took $\Lambda/\Lambda_{\rm TC} = 10^5$. The shapes of the scaling relation are qualitatively similar. We also find that the analytical expression (56) is close to the numerical solution for the two-loop gauge coupling (28), which will be discussed in the next subsection.

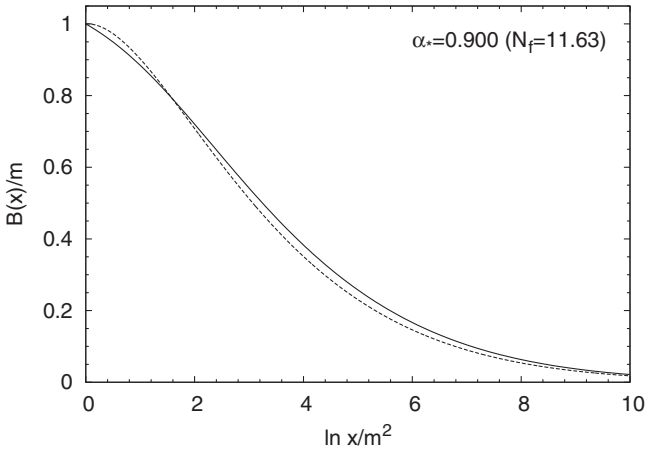

FIG. 5. Behaviors of the mass function in the parabolic approximation. The solid and dashed curves correspond to the numerical solution of the improved ladder SD Eq. (39) with the running gauge coupling (46) and the bifurcation solution (47), respectively. We took $N_{\rm TC} = 3$ and $N_f = 11.63$, which yields $\alpha_* = 0.900$ and $\lambda_* = 0.287$.

C. Numerical solution for the improved ladder SD equation with the two-loop gauge coupling

We studied the parabolic approximation in the analytical and numerical ways, so far.

Let us now solve numerically the improved ladder SD equation with the gauge coupling (28) expressed through

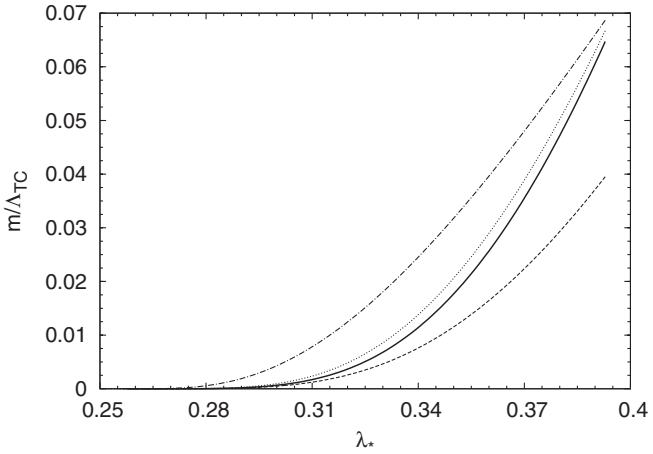

FIG. 6. Scaling relations in several approaches. The solid, dashed, and dash-dotted curves correspond to the numerical solution of the ladder SD Eq. (39) for the two-loop β function, the parabolic approximation, and the fixed coupling, respectively. The dotted one is for the analytical expression (56) in the parabolic approximation. We took $N_{\rm TC} = 3$ and varied continuously N_f.

the Lambert function. We calculate the Lambert function via the Halley's method [32],

$$w_{j+1} = w_j - \frac{w_j e^{w_j} - z}{e^{w_j}(w_j + 1) - \frac{(w_j+2)(w_j e^{w_j} - z)}{2w_j+2}}. \quad (66)$$

The computational technique for solving the improved ladder SD equation is described in Ref. [35]. The results are depicted in Figs. 6–13. We also show the results for the fixed gauge coupling $\lambda(x) = \lambda_*$. In this case, we take the UV cutoff Λ of the SD equation to $\Lambda_{\rm TC}$. We confirmed that the consequences of the fixed gauge coupling are consistent with those in Ref. [21], where $\lambda(x) = \lambda_* \theta(\Lambda_{\rm TC}^2 - x)$ was essentially used, instead of the two-loop one (28).

We depict the scaling relation in Fig. 6. We confirmed that the numerical solution for the two-loop gauge coupling (28) is unchanged for $\Lambda/\Lambda_{\rm TC} = 10^{2,\cdots,10}$. (It is not the case for $\Lambda/\Lambda_{\rm TC} = 10^{0,1}$, however.) In the figure, we took $\Lambda/\Lambda_{\rm TC} = 10^5$. We find that the numerical values of the dynamical mass $m/\Lambda_{\rm TC}$ for the two-loop gauge coupling is smaller than those for the fixed coupling. It is amazing that the analytic solution for the parabolic approximation is quantitatively close to the numerical one for the two-loop gauge coupling.

In Fig. 7, we show the behaviors of the mass functions for the two-loop gauge coupling, the parabolic approximation, and the fixed gauge coupling. In this resolution, we cannot distinguish each other. We did not draw here the analytical solution (47) for the parabolic approximation. Although the behavior is close to the numerical one, there is a slight deviation between the analytical and three numerical solutions. Compare Fig. 5 with Fig. 7. An important point is that we normalized the mass function by the dynamical mass $B(x = m^2) = m$, not by $\Lambda_{\rm TC}$. Note that the dynamical masses for the two-loop gauge coupling, the parabolic approximation, and the fixed gauge coupling are numerically obtained as $m/\Lambda_{\rm TC} = 1.08 \times 10^{-4}$, 0.845×10^{-4}, 13.3×10^{-4} for $N_{\rm TC} = 3$ and $N_f = 11.63$, respectively. If we had normalized $B(x)$ by $\Lambda_{\rm TC}$, the three behaviors would thus look very different. Owing to this universal nature of the dimensionless mass function normalized by the dynamical mass, $B(x)/m$, the normalized physical quantities such as the decay constant F_π/m, the vacuum energy $\langle\theta^\mu_\mu\rangle/m^4$, and the technigluon condensate $\langle G^2_{\mu\nu}\rangle/m^4$, which are determined through the mass function, become insensitive to the approximations of the running gauge coupling near the conformal edge, as we will see later.

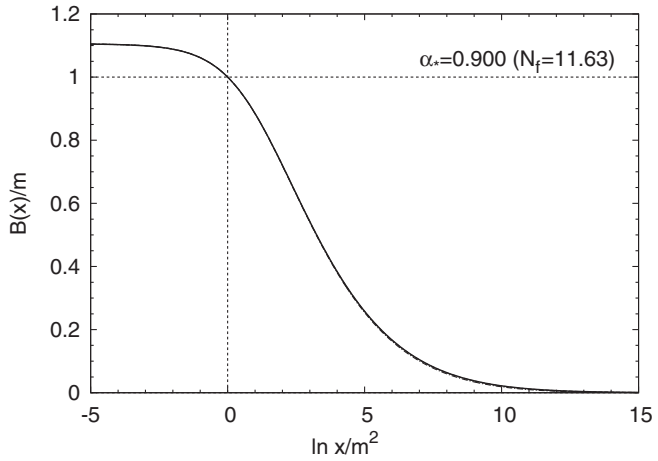

FIG. 7. Behaviors of the mass function in the numerical approaches. The bold solid, dashed, and dash-dotted curves correspond to the numerical solutions of the improved ladder SD equation for the two-loop β function, the parabolic approximation, and the fixed coupling, respectively. We normalized each scale by each dynamical mass $B(x = m^2) = m$. We took $N_{\rm TC} = 3$ and $N_f = 11.63$, which yields $\alpha_* = 0.900$ and $\lambda_* = 0.287$. In this resolution, we cannot distinguish each other, however.

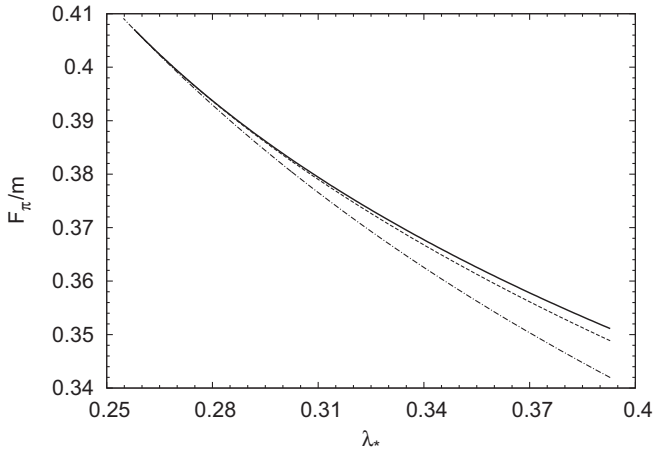

FIG. 8. Decay constant F_π in the numerical approaches. The solid, dashed, and dash-dotted curves correspond to the numerical solution of the ladder SD Eq. (39) for the two-loop β function, the parabolic approximation, and the fixed coupling, respectively. We took $N_{\rm TC} = 3$ and $N_D = 1$.

How about the relation between the scale $\alpha(\mu^2 = \mu_{\rm cr}^2) = \alpha_{\rm cr}$ and the dynamical mass m? By definition, we can obtain the scale $\mu_{\rm cr}$ by

$$W(z_{\rm cr}) = 4\lambda_* - 1, \quad (67)$$

with

$$z_{\rm cr} \equiv e^{-1}\left(\frac{\mu_{\rm cr}^2}{\Lambda_{\rm TC}^2}\right)^{b_0\alpha_*}. \quad (68)$$

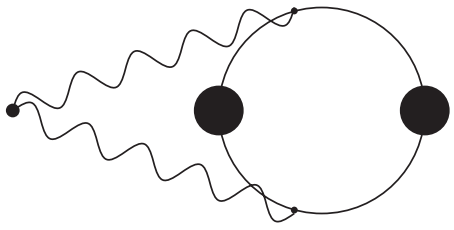

FIG. 9. Technigluon condensate associated with the generation of mass m.

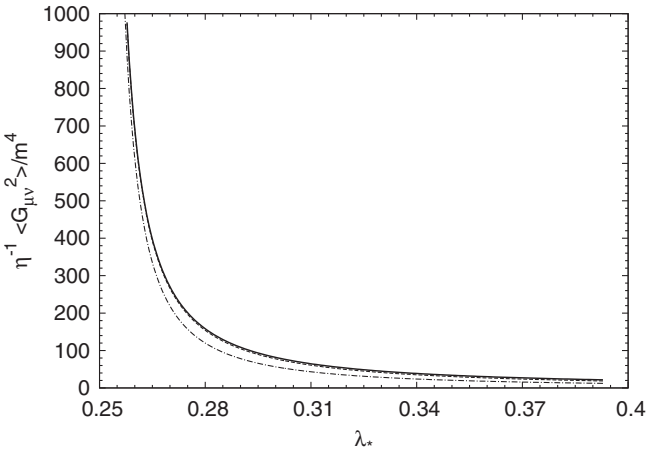

FIG. 10. Behaviors of the gluon condensate in the numerical approaches. The solid, dashed and dash-dotted curves correspond to the numerical solution of the ladder SD Eq. (39) for the two-loop β function, the parabolic approximation, and the fixed coupling, respectively. The factor η is defined by $\eta \equiv N_{\rm TC}N_f/(2\pi^2)$. We took $N_{\rm TC} = 3$. The cutoff is $\Lambda/\Lambda_{\rm TC} = 10^5$ for the two-loop β function and the parabolic approximation. For the fixed gauge coupling, the cutoff is taken as $\Lambda = \Lambda_{\rm TC}$.

For $N_{\rm TC} = 3$ and $N_f = 11.63$, the scale $\alpha(\mu^2 = \mu_{\rm cr}^2) = \alpha_{\rm cr}$ is numerically obtained as $\mu_{\rm cr}/\Lambda_{\rm TC} = 0.189$. As we showed previously, the dynamical mass is $m/\Lambda_{\rm TC} \simeq 1.08 \times 10^{-4}$. When we vary the number of flavor to $N_f = 11.85$, they are much more hierarchical, $\mu_{\rm cr}/\Lambda_{\rm TC} = 0.00225$ and $m/\Lambda_{\rm TC} \simeq 5.88 \times 10^{-10}$. In the parabolic approximation, we find a more handy formula,

$$\mu_{\rm cr} = e^{(1/2s)(\ln\tilde{\omega}+1)}\Lambda_{\rm TC}. \tag{69}$$

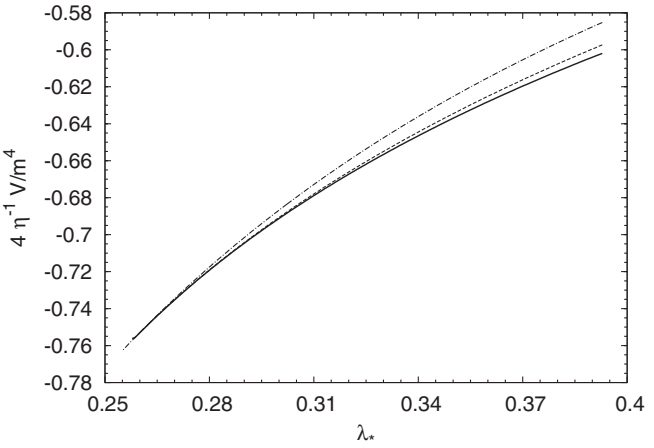

FIG. 11. Behaviors of the vacuum energy in the numerical approaches. The solid, dashed, and dash-dotted curves correspond to the numerical solutions of the ladder SD Eq. (39) for the two-loop β function, the parabolic approximation, and the fixed coupling, respectively. The factor η is defined by $\eta \equiv N_{\rm TC}N_f/(2\pi^2)$. We took $N_{\rm TC} = 3$.

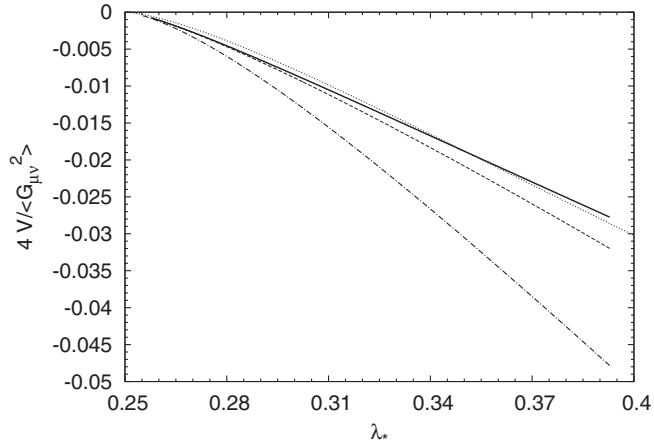

FIG. 12. Ratio of the vacuum energy and the technigluon condensate. The solid, dashed, and dash-dotted curves correspond to the numerical solutions of the ladder SD Eq. (39) for the two-loop β function, the parabolic approximation, and the fixed coupling, respectively. We took $N_{\rm TC} = 3$. The dotted line corresponds to the least-squares fitting by $\xi\tilde{\omega}^3/\lambda_*$. Numerically, we obtain $\xi \simeq -0.026$.

This is apparently much larger than the dynamical mass m in Eq. (58),

$$m \sim e^{((-\pi)/\tilde{\omega})}\Lambda_{\rm TC}. \tag{70}$$

We show a concrete value for $N_{\rm TC} = 3$ and $N_f = 11.85$ in Fig. 3.

Let us calculate the decay constant F_π of the technipion, which is connected with the weak boson mass. We assume that a part of the fermion flavor N_f couples to the electroweak current. In order to estimate the decay constant, we employ the Pagels-Stokar formula [36],

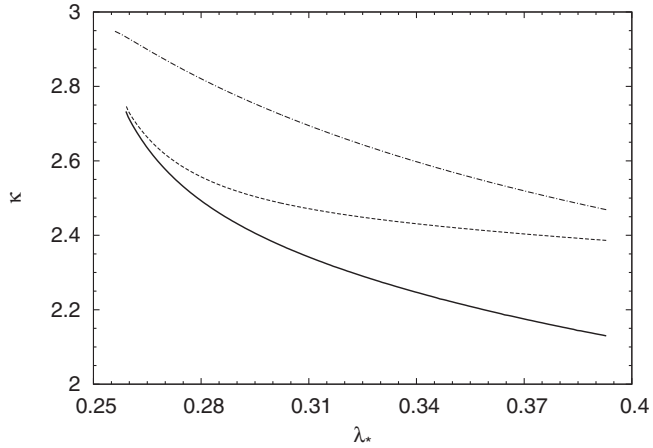

FIG. 13. Instantaneous exponent of the nonperturbative beta function with respect to $\tilde{\omega}$. The vertical axis at $\lambda_* = 1/4 = 0.25$ is the criticality (conformal edge). The solid, dashed and dash-dotted curves correspond to the numerical solutions of the ladder SD Eq. (39) for the two-loop β function, the parabolic approximation, and the fixed coupling, respectively.

$$F_\pi^2 = \frac{N_D N_{\rm TC}}{4\pi^2}\int_0^{\Lambda^2} dx x \frac{B^2(x) - \frac{x}{4}\frac{d}{dx}B^2(x)}{[x + B^2(x)]^2}, \quad (71)$$

where N_D denotes the number of fermion doublets which couple to the electroweak current. The numerical results for the two-loop gauge coupling, the parabolic approximation, and the fixed gauge coupling are shown in Fig. 8. We found that the parabolic approximation works well. Note that $F_\pi/m \simeq 0.41 \times \sqrt{N_D N_{\rm TC}/3}$ near the critical coupling, where we took into account the dependence of $N_{\rm TC}$ and N_D. Thus, when we fix $F_\pi = 246$ GeV, we can estimate the dynamical mass as $m \sim 1\ {\rm TeV}/\sqrt{N_D N_{\rm TC}}$.

The nonperturbative technigluon condensate defined in Eq. (35) can be estimated as [37]

$$\langle G_{\mu\nu}^2 \rangle = \frac{N_{\rm TC} N_f}{2\pi^2}\int_0^{\Lambda^2} dx x \frac{B^2(x)}{x + B^2(x)}. \quad (72)$$

See also Fig. 9. Note that after substituting the solution of the ladder SD equation, the expression of $\langle G_{\mu\nu}^2 \rangle$ explicitly depends only on the mass function $B(x)$ and has no explicit dependence of the running of the gauge coupling [37]. Hence we expect that the result is not sensitive to the details of the running behaviors of the gauge coupling: The numerical results for the two-loop gauge coupling, the parabolic approximation, and the fixed gauge coupling are shown in Fig. 10. We found that the behavior of $\langle G_{\mu\nu}^2 \rangle$ is *not* like $\langle G_{\mu\nu}^2 \rangle \sim m^4$ as assumed in Refs. [2,27], but $\langle G_{\mu\nu}^2 \rangle/m^4 \sim 1/\tilde{\omega}^3 \to \infty$ in the limit of $\lambda_* \to \lambda_{\rm cr}$. Our result directly confirms the estimate of the technigluon condensate made in Ref. [23] which assumed the ladder result for the vacuum energy Eq. (10) and nonperturbative beta function Eq. (4) in the case of the nonrunning coupling. We can show this behavior by using the approximation (59), i.e.,

$$\langle G_{\mu\nu}^2 \rangle \simeq \frac{N_{\rm TC} N_f}{2\pi^2}\int_{m^2}^{\Lambda_{\rm TC}^2} dx B^2(x), \quad (73)$$

and thus

$$\langle G_{\mu\nu}^2 \rangle \simeq \frac{N_{\rm TC} N_f}{2\pi^2}\frac{1+\tilde{\omega}^2}{\tilde{\omega}^2} m^4 \ln\left(\frac{\Lambda_{\rm TC}}{m}\right) \sim \frac{N_{\rm TC} N_f}{2\pi}\frac{m^4}{\tilde{\omega}^3}, \quad (74)$$

where we used the scaling relation (58).

Next to the vacuum energy $V = \langle \theta_\mu^\mu \rangle/4$ as defined in Eq. (35). Substituting the solution $B_{\rm sol}(x)$ of the ladder SD Eq. (39) for the CJT potential (37), we obtain the vacuum energy,

$$V = V_{\rm CJT}(B = B_{\rm sol}), \quad (75)$$

$$= -\frac{N_{\rm TC} N_f}{8\pi^2}\int_0^{\Lambda^2} dx x \left[\ln\left(1 + \frac{B_{\rm sol}^2(x)}{x}\right) - \frac{B_{\rm sol}^2(x)}{x + B_{\rm sol}^2(x)}\right], \quad (76)$$

where we explicitly wrote the subscript for the mass function in order to distinguish the vacuum energy from the CJT potential itself. [Of course, also in the expressions (71) and (72), $B(x)$ represents $B(x) = B_{\rm sol}(x)$.] The numerical results for the two-loop gauge coupling, the parabolic approximation, and the fixed gauge coupling are shown in Fig. 11. It is clear that the vacuum energy normalized by m^4 does not vanish, because the numerical calculations shown in Fig. 11 suggests

$$\langle \theta_\mu^\mu \rangle = 4V \simeq -0.76\eta m^4, \quad \text{with} \quad \eta \equiv \frac{N_{\rm TC} N_f}{2\pi^2}, \quad (77)$$

near the critical coupling. This result disagrees with the assumption in Refs. [2,27].

The approximate expression (59) suggests that our results coincide with the estimate of V for the fixed gauge coupling [9]:

$$4V \simeq -\frac{4N_{\rm TC} N_f}{\pi^4} m^4 = -0.81\eta m^4. \quad (78)$$

It is to be noted that this value is also close to the numerical estimate (77) in our case. In fact, although the CJT potential itself explicitly depends on the running of the gauge coupling, the vacuum energy has an explicit dependence only on the mass function $B_{\rm sol}(x)$ after using the solution of the SD equation, and hence only depends implicitly on the running gauge coupling through $B_{\rm sol}(x)$. [Compare Eq. (37) with Eq. (76).] The IR behaviors of $B_{\rm sol}(x)$ for the two-loop running and fixed couplings coincide each other, as shown in Fig. 7. (Inside of the frame of the figure corresponds to the IR region.) Since the UV contribution to the vacuum energy is negligible, the vacuum energy (77) for the two-loop running gauge coupling is almost the same as that for the nonrunning one.

From these analytical and numerical analyses, we conclude that in the vacuum energy there is no divergence unlike the technigluon condensate, $\langle G_{\mu\nu}^2 \rangle/m^4 \to \infty$, and also the quantity V/m^4 does not approach to zero in the limit of $\lambda_* \to \lambda_{\rm cr}$, within our approximation.

Since the formal RG analysis yields [18]

$$\langle \theta_\mu^\mu \rangle = 4V = \frac{\beta}{4\alpha}\langle G_{\mu\nu}^2 \rangle, \quad (79)$$

the ratio $4V/\langle G_{\mu\nu}^2 \rangle$ is closely connected with the β function. We depict it in Fig. 12. By using the least-squares method, we numerically obtain

$$\frac{\beta}{4\alpha} = \frac{4V}{\langle G_{\mu\nu}^2 \rangle} = \xi\frac{\tilde{\omega}^3}{\lambda_*}, \quad \text{with} \quad \xi = -0.026. \quad (80)$$

in the form similar to the nonrunning case. In the case of the nonrunning coupling $\lambda(x) = \lambda_*$, we have the analytical result $\xi = -1/(8\pi) = -0.0398$ corresponding to Eq. (4), $\beta = -2\tilde{\omega}^3/(3C_F)$, which agrees with the numerical result $\xi = -0.0400$ in the vicinity of the critical coupling. Incidentally, in the case of the two-loop coupling we may

take a fitting function other than the above: $\xi(1/\lambda_{\rm cr} - 1/\lambda_*)^{3/2}$ with $\xi = -0.0155$, which yields much better fitting.

How about the exponent of the nonperturbative beta function with respect to $\tilde{\omega}$? Let us write

$$\frac{\beta}{4\alpha} = \frac{4V}{\langle G_{\mu\nu}^2 \rangle} = f(\lambda_*)\tilde{\omega}^{\kappa}, \tag{81}$$

where $f(\lambda_*)$ represents some function of λ_* and the instantaneous exponent $\kappa = \kappa(\lambda_*)$ is extracted from the relation

$$\kappa = \frac{\tilde{\omega}\frac{\partial}{\partial\tilde{\omega}}(\frac{\beta}{4\alpha})}{(\frac{\beta}{4\alpha})}. \tag{82}$$

We depict the numerical results in Fig. 13. Near the critical edge, the numerical values of $\kappa = \kappa(\lambda_*)$ are

$$\kappa \simeq 2.73, 2.75, 2.95, \tag{83}$$

for the two-loop exact solution, the parabolic approximation and the fixed coupling case, respectively. Because the linear and multiple zeros of the beta function with respect to $\alpha(\mu) = \alpha \simeq \alpha_*$ correspond to $\kappa|_{\lambda_*=\lambda_{\rm cr}} = 2$ and $\kappa|_{\lambda_*=\lambda_{\rm cr}} > 2$, respectively, the numerical results obviously show that the nonperturbative beta function has the multiple zero at the critical edge. If we smoothly extrapolate the behavior of κ to the criticality, the behavior of the nonperturbative beta function at the criticality will be $\beta \propto -\tilde{\omega}^3$, in accord with the above least-square fitting (80).

It is noticeable that the nonperturbative beta function has a multiple zero at the critical coupling $\alpha \simeq \alpha_* = \alpha_{\rm cr}$, as shown in Eq. (80), which corresponds to the essential singularity scaling Eq. (58). On the other hand, it is not the case in the perturbative (two-loop) expression (22), which has a linear zero, $\beta \sim \alpha - \alpha_* \sim \alpha_{\rm cr} - \alpha_*$ at criticality $\alpha = \alpha_{\rm cr}$. Therefore the actual beta function is crucially different from the perturbative beta function which should be modified in the IR region where the nonperturbative dynamics responsible for the mass generation is dominant. The full β function including the perturbative and the nonperturbative contributions is thus suggested in Fig. 14. We hope that the lattice studies will clarify this nature.

Now we discuss the behavior of the TD mass in the limit toward the criticality. Through the PCDC, Eq. (9), the vacuum energy is connected with the TD mass,

$$F_{\rm TD}^2 M_{\rm TD}^2 = -d_\theta \langle \theta_\mu^\mu \rangle = -4 d_\theta V, \tag{84}$$

where $F_{\rm TD}$, $M_{\rm TD}$ and $d_\theta (= 4)$ represent the TD decay constant, the TD mass and the scale dimension of the trace of the energy-momentum tensor. Our results qualitatively agree with the conclusion in the case of SD equation with the nonrunning gauge coupling, Eq. (12), which is in disagreement with Refs. [2,27]: There is no true (massless) NG boson for the conformal symmetry at the criticality,

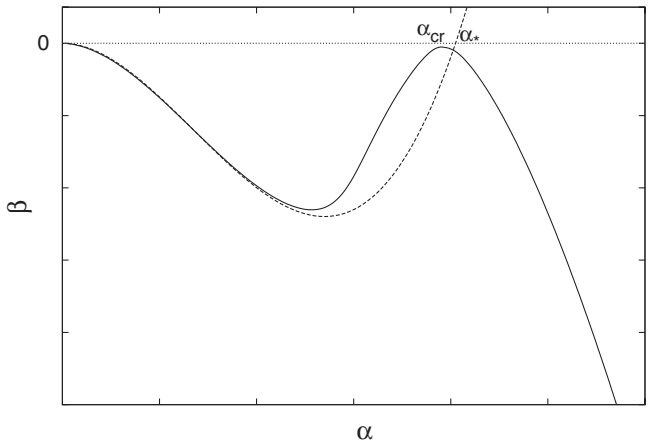

FIG. 14. Conjecture of the shape of the β function including the nonperturbative behavior. The bold solid and dashed curves correspond to the conjectured β function and the purely perturbative one, respectively.

unless the TD decay constant diverges, i.e., gets decoupled. Such a decoupled TD was in fact implied by the idealized limit of the holographic TD [23]. In the realistic situation of the TC model building $m/\Lambda_{\rm TC}$ is not arbitrarily small but only $m/\Lambda_{\rm TC} \sim m/\Lambda_{\rm ETC} \sim 10^{-3} - 10^{-4}$, so that the ''masslessness'' and ''decoupling'' are somewhat milder. In the quantitative sense our results, though valid only in the vicinity of criticality, indicate rough idea about the mass and decay constant of TD as follows. Substituting our numerical result, Eq. (77), into Eq. (84), we find

$$M_{\rm TD}^2 \simeq 3.02\eta \frac{m^4}{F_{\rm TD}^2}. \tag{85}$$

Furthermore, by using $F_\pi/m \simeq 0.41\sqrt{N_D N_{\rm TC}/3}$ in Eq. (71), we obtain

$$\frac{M_{\rm TD}}{F_\pi} \simeq 3.5 \frac{F_\pi}{F_{\rm TD}} \cdot \left(\sqrt{\frac{N_f}{2N_D}}\sqrt{\frac{8}{2N_D}}\sqrt{\frac{2}{N_{\rm TC}}}\right). \tag{86}$$

The TD with mass, say $M_{\rm TD} \sim 500$ GeV, would require TD coupling smaller than that of the standard model Higgs by $F_\pi/F_{\rm TD} \simeq 3/5$ up to model-dependent factors of N_f, N_D and $N_{\rm TC}$ besides other dynamical details. If the TD mass is much smaller, $F_{\rm TD} \ll F_\pi$, on the other hand, it could lead to a decoupled TD, which might be a candidate of dark matter. Detailed studies are required in order to confirm whether or not such a decoupled TD satisfies conditions for dark matter.

IV. SUMMARY AND DISCUSSION

We have studied analytically the improved ladder SD equation with the parabolic approximation for the beta function and also analyzed numerically the solution of the ladder SD equation with the two-loop exact running gauge coupling.

We explicitly calculated the technigluon condensate near the conformal edge and found that the behavior is $\langle G^2_{\mu\nu}\rangle/m^4 \sim (\alpha/\alpha_{\rm cr}-1)^{-3/2} \to \infty$ $(\alpha \to \alpha_{\rm cr})$ with $m \ll \Lambda_{\rm TC}$, in accord with Ref. [23] but in disagreement with the assumption of Refs. [2,27]. The numerical calculation is consistent with this analytic result. This situation is different from QCD having no approximate conformal symmetry, where $\Lambda_{\rm QCD} \sim m$ and $\langle G^2_{\mu\nu}\rangle_{\rm full} \sim \langle G^2_{\mu\nu}\rangle_{\rm perturbative} \sim \Lambda^4_{\rm QCD}$.

On the other hand, the vacuum energy (divided by m^4) is finite, $V/m^4 \to$ const, even in the critical limit, as in the case of the fixed gauge coupling. Our result for the vacuum energy only yields a combination of the mass $M_{\rm TD}$ and the decay constant $F_{\rm TD}$ through PCDC but not each of them separately, as was the case for most of the discussions in the literature. Combining the PCDC relation, Eq. (84), $F^2_{\rm TD}M^2_{\rm TD} = -4\langle\theta^\mu_\mu\rangle$, with the numerical result for the vacuum energy, Eq. (77), we found $M^2_{\rm TD} = 3.02\eta m^4/F^2_{\rm TD}$ with $\eta \equiv N_{\rm TC}N_f/(2\pi^2)$, Eq. (85). This relation implies $M_{\rm TD}/m \sim m/F_{\rm TD}$ near the conformal edge and hence naturally $M_{\rm TD} = \mathcal{O}(m)$ in contrast to Refs. [27,28]. (A similar conclusion was made in a different context [38].) As an extreme possibility we could have $M_{\rm TD}/m \to 0$ only when $m/F_{\rm TD} \to 0$ and the TD gets decoupled. If such an idealized decoupled massless TD is realized at the conformal edge, the light decoupled TD as a pseudo NG boson slightly off the conformal edge may be a candidate for the dark matter.

The scale anomaly formally yields the relation $\beta/(4\alpha) = \langle\theta^\mu_\mu\rangle/\langle G^2_{\mu\nu}\rangle$, so that the above results imply the nonperturbative behavior of the beta function reflecting the nonperturbative effects of the dynamical mass generation, $\beta(\alpha) \sim -(\alpha/\alpha_{\rm cr}-1)^{3/2}$. Numerically, we obtained $\beta/(4\alpha) = \xi(\alpha/\alpha_{\rm cr}-1)^{3/2}/\lambda_*$ with $\xi = -0.026$ for the two-loop running gauge coupling. The absolute value of the coefficient is smaller than that for the fixed gauge coupling, $\xi = -0.04$. However, the exponent κ of the nonperturbative beta function at the conformal edge seems universal, $\kappa = 3$, where $\beta/(4\alpha) \propto (\alpha/\alpha_{\rm cr}-1)^{\kappa/2}$. This nature of the nonperturbative beta function having the multiple zero is crucial to reproduce the essential singularity scaling Eq. (58).

We have settled some of the controversy related with the TD mass raised within the improved ladder SD equation. However, several issues remain to be explored:

In particular, a central problem is how large the TD mass $M_{\rm TD}$ is. In order to discuss collider phenomenology of the TD and also check whether or not a decoupled TD is in fact realized near the conformal edge, we should obtain mass $M_{\rm TD}$ and the decay constant $F_{\rm TD}$ separately.

Thus we would need more information other than the vacuum energy. As was mentioned in the Introduction, such a calculation was in fact done in a most straightforward way [21], based on the SD and BS equations in the improved ladder approximation with the two-loop running coupling constant having the CBZ-IR fixed point, which suggests $M_{\rm TD} \sim \sqrt{2}m$, Eq. (14), without evidence of the decoupled light TD much smaller than m. Note however that this calculation was actually done only numerically and at slightly off the conformal edge, and hence the result is not conclusive about the very close point to the conformal edge.

On the other hand, in the holographic framework [23] which has a wider parameter space than that of the (improved) ladder approximation so as to adjust the S parameter arbitrarily small, it was shown that at the limit of conformal edge $m/\Lambda_{\rm TC} \to 0$ the technigluon condensate vanishes $\Gamma \to \infty$, with Γ parameterized as in Eq. (17), which in turn implies $M_{\rm TD}/m \to 0$ at the sacrifice of decoupling $m/F_{\rm TD} \to 0$, although such an extreme case is unlikely for the realistic setting of the typical TC model building (slightly away from the conformal edge $m/\Lambda_{\rm TC} = 10^{-3} - 10^{-4}$) where the holography suggests $M_{\rm TD}/m = \mathcal{O}(1)$, or $M_{\rm TD} \sim 600$ GeV [Eq. (20)]. So although the theoretical possibility for the decoupled TD at the conformal edge is not completely excluded, there is no signature of such a possibility at least in near conformal edge region relevant to the realistic TC model building.

We have not included interactions like ETC (extended technicolor) between the techni-fermions and the quarks/leptons which should be included to give mass to the quarks and leptons in the realistic TC models. Including these interactions also induce additional interactions among the techni-fermions themselves, which may be described by the effective four-fermion interactions in addition to the TC gauge interactions we have discussed (''gauged NJL model''). Such ETC-like effects on the TD mass were already studied intensively in the ladder SD equation with nonrunning gauge coupling [10,12,13], with the results $M_{\rm TD} \sim \mathcal{O}(m)$, i.e., against very light TD mass and decoupled TD, as was mentioned in the Introduction. As is clear from our arguments in this paper, the situation with the additional four-fermion interaction in the ladder approximation with nonrunning gauge coupling will remain essentially the same in the improved-ladder SD equation with the two-loop running gauge coupling. Moreover, more elaborate calculations in the gauged NJL model [15] showed that $M_{\rm TD} \to \sqrt{2}m$ [Eq. (13)] in such a limit along the whole critical line $(0 < \alpha \le \alpha_{\rm cr})$. Note also that the result Eq. (13) [15] is consistent with Eq. (14) [21] which is the straightforward computation of the spectra within the ladder SD and BS equations in the improved ladder approximation with the two-loop gauge coupling near the conformal edge (without four-fermion coupling). Note however that these calculations did only for the inverse propagator at zero-momentum but not the pole mass (on-shell mass), and hence are still not conclusive. We definitely need more reliable calculations such as the lattice simulations about the TD spectrum.

We have considered TD as a bound state of technifermion and anti-technifermion both of which acquired mass m. The mass m spontaneously breaks chiral symmetry and

at the same time breaks spontaneously and explicitly the scale symmetry, the scale anomaly due to this mass generation being of order $\mathcal{O}(m^4)$ as we computed explicitly in this paper. Hence such a bound state should have mass of order $\mathcal{O}(m)(\ll \Lambda_{\rm TC})$. On the contrary, it was argued [23] that the technigliteball mass should be of order $\mathcal{O}(\Lambda_{\rm TC})$, since the scale-symmetry breaking free from the technifermion mass generation is due to the scale anomaly of order $\mathcal{O}(\Lambda_{\rm TC}^4)$ corresponding to the usual perturbative running of the coupling for $\mu > \Lambda_{\rm TC}$ ($\langle\theta^\mu_\mu\rangle_{\rm perturbative}$ in Eq. (35)). Then we expect little mixing between our TD and the technigliteball, in sharp contrast to QCD where the flavor-single scalar meson (analogue of TD) and the scalar glueball may mix strongly. More reliable calculations are of course highly desired.

In this paper, we assumed that the fermion loop is dominant in the technigluon condensate and the vacuum energy. In principle, there might exist nonperturbative technigluonic effects. It is difficult to estimate it in our approach, however. A lattice simulation may also resolve this issue. We shed a light on the problem which has made confusion in the improved ladder approximation with the two-loop running gauge coupling. We clarified it in the analytical and numerical ways within the same framework of the improved ladder SD approximation. There should exist nonperturbative effects beyond the improved ladder approximation, although it is very unclear whether or not they are relevant. Toward a conclusive answer, one might challenge a more rigorous approach such as a lattice gauge theory. We hope that our results will be reconfirmed more rigorously in future.

Needless to say, our analysis in this paper is also applicable to dynamical symmetry breaking scenarios with large anomalous dimension/conformality other than TC, such as the top-mode standard model with extra dimensions which has a UV fixed point [35], higher representation quark condensate model [39], or even the QCD with finite temperature where the running of the coupling will be frozen (mocking conformal) in the IR region below the temperature scale, etc..

ACKNOWLEDGMENTS

The authors thank T. Appelquist and T. Kugo for fruitful discussions. M. H. was supported by Maskawa Institute for Science and Culture, Kyoto Sangyo University. This work was supported in part by the JSPS Grant-in-Aid for Scientific Research (S) under Grant No. 22224003.

[1] K. Yamawaki, M. Bando, and K. Matumoto, Phys. Rev. Lett. **56**, 1335 (1986); See also M. Bando, T. Morozumi, H. So, and K. Yamawaki, Phys. Rev. Lett. **59**, 389 (1987).
[2] M. Bando, K. Matumoto, and K. Yamawaki, Phys. Lett. B **178**, 308 (1986).
[3] T. Maskawa and H. Nakajima, Prog. Theor. Phys. **52**, 1326 (1974); **54**, 860 (1975).
[4] B. Holdom, Phys. Rev. D **24**, 1441 (1981).
[5] T. Akiba and T. Yanagida, Phys. Lett. **169B**, 432 (1986); T. W. Appelquist, D. Karabali, and L. C. R. Wijewardhana, Phys. Rev. Lett. **57**, 957 (1986); T. Appelquist and L. C. R. Wijewardhana, Phys. Rev. D **36**, 568 (1987); For an earlier work on this line based on a pure numerical analysis, see B. Holdom, Phys. Lett. **150B**, 301 (1985).
[6] C. T. Hill and E. H. Simmons, Phys. Rep. **381**, 235 (2003); **390**, 553(E) (2004); K. Yamawaki, arXiv:hep-ph/9603293.
[7] R. Fukuda and T. Kugo, Nucl. Phys. **B117**, 250 (1976).
[8] V. A. Miransky, Nuovo Cimento Soc. Ital. Fis. A **90**, 149 (1985).
[9] V. A. Miransky and V. P. Gusynin, Prog. Theor. Phys. **81**, 426 (1989).
[10] W. A. Bardeen, C. N. Leung, and S. T. Love, Phys. Rev. Lett. **56**, 1230 (1986); C. N. Leung, S. T. Love, and W. A. Bardeen, Nucl. Phys. **B323**, 493 (1989).
[11] B. Holdom and J. Terning, Phys. Lett. B **187**, 357 (1987); Phys. Lett. B **200**, 338 (1988).
[12] K. i. Kondo, H. Mino, and K. Yamawaki, Phys. Rev. D **39**, 2430 (1989); K. Yamawaki, in *Proc. Johns Hopkins Workshop on Current Problems in Particle Theory 12, Baltimore, June 8–10 1988*, edited by G. Domokos and S. Kovesi-Domokos (World Scientific Pub. Co., Singapore, 1988).
[13] T. Nonoyama, T. B. Suzuki, and K. Yamawaki, Prog. Theor. Phys. **81**, 1238 (1989).
[14] K. Yamawaki, Prog. Theor. Phys. Suppl. **180**, 1 (2009); Int. J. Mod. Phys. A **25**, 5128 (2010).
[15] S. Shuto, M. Tanabashi, and K. Yamawaki, in *Proceedings of the 1989 Workshop on Dynamical Symmetry Breaking, Dec. 21–23, 1989*, Nagoya, edited by T. Muta and K. Yamawaki (Nagoya University, Nagoya, 1990) p. 115; M. S. Carena and C. E. M. Wagner, Phys. Lett. B **285**, 277 (1992); M. Hashimoto, Phys. Lett. B **441**, 389 (1998).
[16] K. D. Lane and M. V. Ramana, Phys. Rev. D **44**, 2678 (1991).
[17] T. Appelquist, J. Terning, and L. C. Wijewardhana, Phys. Rev. Lett. **77**, 1214 (1996); T. Appelquist, A. Ratnaweera, J. Terning, and L. C. Wijewardhana, Phys. Rev. D **58**, 105017 (1998).
[18] V. A. Miransky and K. Yamawaki, Phys. Rev. D **55**, 5051 (1997); **56**, 3768(E) (1997).
[19] W. E. Caswell, Phys. Rev. Lett. **33**, 244 (1974); T. Banks and A. Zaks, Nucl. Phys. **B196**, 189 (1982).
[20] K. Yamawaki, Prog. Theor. Phys. Suppl. **167**, 127 (2007).
[21] M. Harada, M. Kurachi, and K. Yamawaki, Phys. Rev. D **68**, 076001 (2003).

[22] M. Kurachi and R. Shrock, J. High Energy Phys. 12 (2006) 034.
[23] K. Haba, S. Matsuzaki, and K. Yamawaki, Phys. Rev. D **82**, 055007 (2010); arXiv:1006.2526.
[24] M. E. Peskin and T. Takeuchi, Phys. Rev. Lett. **65**, 964 (1990); B. Holdom and J. Terning, Phys. Lett. B **247**, 88 (1990); M. Golden and L. Randall, Nucl. Phys. **B361**, 3 (1991).
[25] K. Haba, S. Matsuzaki, and K. Yamawaki, Prog. Theor. Phys. **120**, 691 (2008).
[26] M. Harada, M. Kurachi, and K. Yamawaki, Prog. Theor. Phys. **115**, 765 (2006); M. Kurachi and R. Shrock, Phys. Rev. D **74**, 056003 (2006); M. Kurachi, R. Shrock, and K. Yamawaki, Phys. Rev. D **76**, 035003 (2007).
[27] T. Appelquist and Y. Bai, Phys. Rev. D **82**, 071701 (2010).
[28] D. D. Dietrich, F. Sannino, and K. Tuominen, Phys. Rev. D **72**, 055001 (2005).
[29] V. A. Miransky, Yad. Fiz. **38**, 468 (1983) [Sov. J. Nucl. Phys. **38**, 280 (1983)]; K. Higashijima, Phys. Rev. D **29**, 1228 (1984).
[30] C. Amsler *et al.* (Particle Data Group), Phys. Lett. B **667**, 1 (2008).
[31] E. Gardi and M. Karliner, Nucl. Phys. **B529**, 383 (1998); E. Gardi, G. Grunberg, and M. Karliner, J. High Energy Phys. 07 (1998) 007.
[32] R. M. Corless, G. H. Gonnet, D. E. G. Hare, D. J. Jeffrey, and D. E. Knuth, Adv. Comput. Math. **5**, 329 (1996).
[33] V. A. Miransky, *Dynamical Symmetry Breaking in Quantum Field Theories* (World Scientific, Singapore, 1993).
[34] D. Atkinson, J. Math. Phys. (N.Y.) **28**, 2494 (1987).
[35] M. Hashimoto, M. Tanabashi, and K. Yamawaki, Phys. Rev. D **64**, 056003 (2001).
[36] H. Pagels and S. Stokar, Phys. Rev. D **20**, 2947 (1979).
[37] V. P. Gusynin, V. A. Kushnir, and V. A. Miransky, Phys. Rev. D **39**, 2355 (1989); **41**, 3279(E) (1990).
[38] L. Vecchi, arXiv:1007.4573.
[39] W. J. Marciano, Phys. Rev. D **21**, 2425 (1980).